EUROPEAN ORGANIZATION FOR NUCLEAR RESEARCH
European Laboratory for Particle Physics

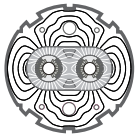

Large Hadron Collider Project

LHC Project Report 16

Transverse Instabilities in the LHC

J. Scott Berg*

Abstract

I first summarize the impedance model that I will be using (this is compiled from the work of several other authors). I then use the methods described elsewhere [1] to determine mode coupling thresholds and growth rates of multibunch modes, including the effects of multibunch mode coupling (see [1]). The effects of feedback are also considered.

*CERN–SL Division

Administrative Secretariat
LHC Division
CERN
CH-1211 Geneva 23
Switzerland

Geneva, 10 July 1996

Name	Symbol	Injection	Collision
Ring circumference	L	26658.883 m	
Betatron tune	ν_y	63.31	
Synchrotron tune	ν_s	0.006	0.00212
Frequency slip factor	η	3.430×10^{-4}	3.473×10^{-4}
Revolution frequency	f_0	11.2455 kHz	
Number of bunches	k_B	2835	
Number of bunch places	M	3564	
Proton energy	E	450 GeV	7000 GeV
Circulating beam current	I	0.536 A	
Transverse physical emittance	ϵ	7.82 nm-rad	0.503 nm-rad
r.m.s. bunch length	σ_ℓ	13 cm	7.7 cm

Table 1: Parameters for the LHC; all values are from Annex 1 of [2].

1 Parameters

The relevant machine parameters for computing transverse single- and multibunch modes are given in Tab. 1. Note that the vertical tune value is used throughout this computation. The bunches are assumed to be Gaussian. Parabolic bunches would probably be a better assumption, but the appropriate matrix elements for the method of [1] have not been computed at this point.

2 Impedance Model

2.1 Broadband Impedance

The broadband impedance model I am using here is described in more detail in [3], and is taken exactly from there (including average β-functions). Note that what I am calling "broadband impedance," Ruggiero [3] describes under the categories of space charge impedance, broad-band resonators, low-frequency impedance, beam screen, and pumping slots. I am categorizing as broadband impedance anything which has roughly the same effect on every multibunch mode; a narrow-band impedance would affect the various multibunch modes differently. Finally, note that for the imaginary parts of quantities, Ruggiero's j is the negative of my i.

The total transverse broadband impedance weighted by the β function is plotted in Fig. 1. The contributions to this total impedance are described in the subsections that follow.

2.1.1 Space charge

Space charge gives a negative inductance. The impedance is 5.208 MΩ/m at injection, and 0.335 MΩ/m at collision. The average β-function is taken to be 85 m.

2.1.2 Resonators

There are several devices which are described by resonators of the form

$$Z_\perp(x\omega_R) = \frac{R_{\rm Res}}{x + iQ(1-x^2)}. \tag{1}$$

Here x is the ratio of the frequency to the resonant frequency for this resonator. Table 2 summarizes the parameters for such impedances.

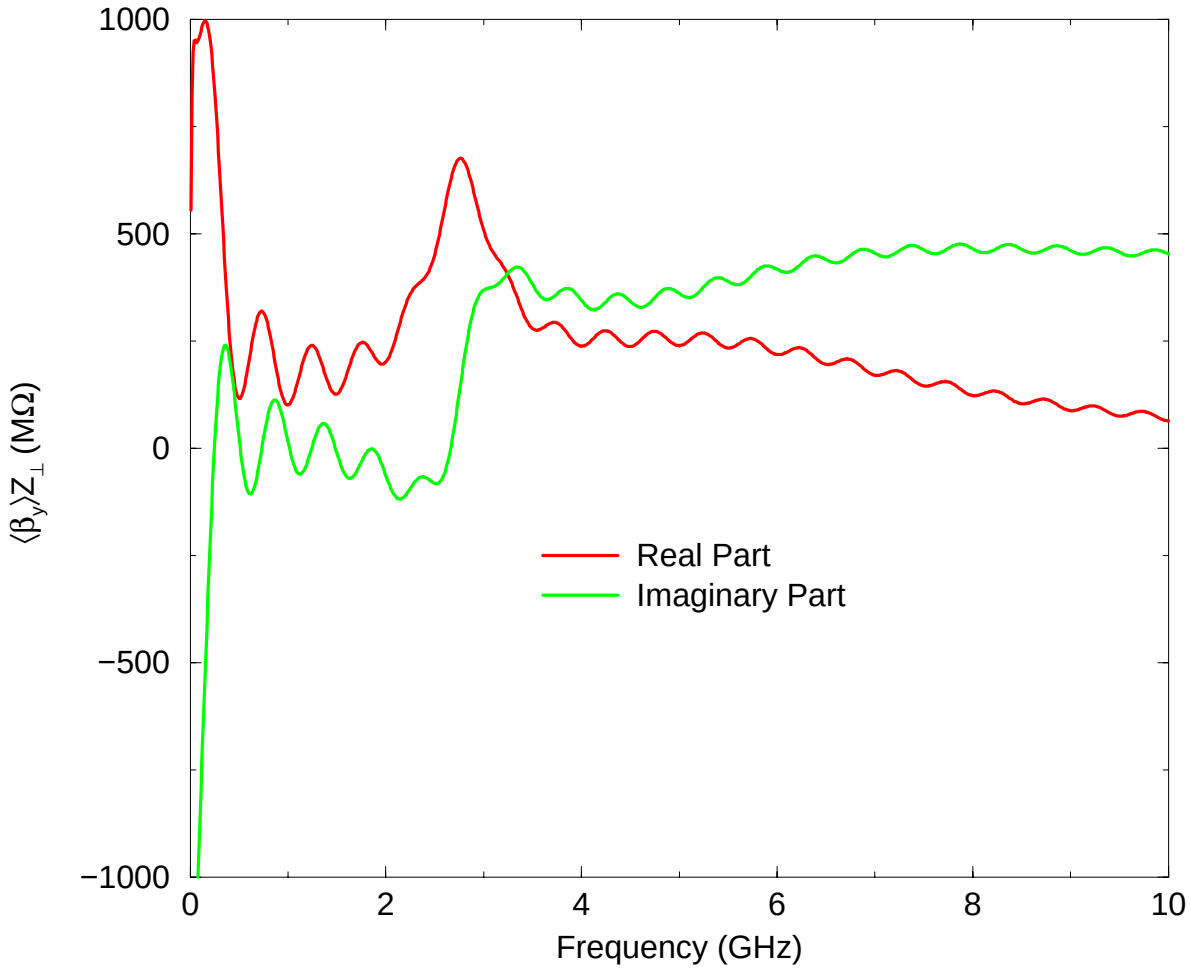

Figure 1: Total transverse broadband impedance for the LHC at injection as described in Sec. 2.1.

Device	$\omega_R/2\pi$	Q	$R_{\rm Res}$	$\langle\beta\rangle$
Shielded bellows (total for 3000)	2.8 GHz	3.5	5.7 MΩ/m	85 m
Monitor tanks (total for 500)	6 GHz	1	1.17 MΩ/m	172.8 m

Table 2: Parameters for devices described by broadband resonators.

2.1.3 Beam position monitors

The impedance from the beam position monitors is given by the formula

$$Z_\perp(\omega) = -i\frac{4\ell}{\pi^2 b^2} N_m Z_s \sin^2\frac{\phi}{2}\frac{\sin(\omega\ell/c)}{\omega\ell/c} e^{i\omega\ell/c}, \qquad (2)$$

where $\ell = 30$ cm, $\phi = 110°$, $Z_s = 50\ \Omega$, $N_m = 500$, and $b = 17.4$ mm. The average β-function is taken to be 172.8 m.

Device	$R_{\rm Ind}$	$\langle\beta\rangle$
Beam screen	0.44 MΩ/m	85 m
Accelerating cavities (total for 8)	3.8 kΩ/m	150 m
Feedback (Septum) cavities (total for 3)	108 kΩ/m	200 m

Table 3: Parameters for devices described by an inductance. The impedance for the septum cavities is computed by taking the $Z_\parallel/n$ of 32 mΩ given in [4] and scaling it by $2R/b^2$, taking b to be 5 cm, the radius of the drift tube [4]. The β-function at the septum cavities is from [5].

2.1.4 Abort kicker magnets

The impedance due to the abort kicker magnets is given by the formula

$$Z_\perp(\omega) = Z_0 \frac{L}{2\pi b^2} \frac{1}{\frac{bd\mu_0\omega}{2\rho_{\rm Ti}} + i\zeta}, \tag{3}$$

where $L = 14 \times 1.26$ m, $b = 14$ mm, $d = 1$ μm, $\rho_{\rm Ti} = 7 \times 10^{-7}$ Ωm, and $\zeta = 2.34$. Note that $Z_0 = 376.73$ Ω is the impedance of free space, and $\mu_0 = 4\pi \times 10^{-7}\Omega{\rm sm}^{-1}$ is the permittivity of free space. The magnets are located in a region where the β-function is about 600 m. Note that Eq. (3) can be written more conveniently as

$$Z_\perp(\omega) = \frac{-iR}{1 - i\omega/\omega_C}, \tag{4}$$

where

$$R = \frac{Z_0 L}{2\pi b^2 \zeta} = 2.306 \text{ MΩ/m} \qquad \omega_C = \frac{2\zeta\rho_{\rm Ti}}{bd\mu_0} = 2\pi \times 29.6 \text{ MHz}. \tag{5}$$

Note that this model for the impedance is probably unphysical, since it leads to a wakefield $W_\perp(\tau)$ which is nonzero at $\tau = 0+$ (in other words, the corresponding longitudinal impedance would lead to a DC beam losing energy).

2.1.5 Purely inductive

There are several devices which are described as purely inductive impedances; their impedance is given by $-iR_{\rm Ind}$. The $R_{\rm Ind}$ for these devices are given in Tab. 3.

2.1.6 Resistive wall

Finally, there is the resistive wall impedance. The beam pipe wall consists of an inner layer of thickness t and resistivity ρ, and an outer layer of thickness t' and resistivity ρ'. For such a pipe, the resistive wall impedance is given by the formula

$$\frac{cL\rho}{\pi\omega b^3}\sqrt{\frac{-i\mu_0\omega}{\rho}}\frac{\tanh\left(t\sqrt{-i\mu_0\omega/\rho}\right) + \sqrt{\rho'/\rho}\tanh\left(t'\sqrt{-i\mu_0\omega/\rho'}\right)}{1 + \sqrt{\rho'/\rho}\tanh\left(t\sqrt{-i\mu_0\omega/\rho}\right)\tanh\left(t'\sqrt{-i\mu_0\omega/\rho'}\right)}, \tag{6}$$

where b is the beam pipe radius, and L is the length of the segment in question.

The ring is taken to consist of two sections: the first has an inner layer of copper, and an outer stainless steel layer. This segment occupies 90% of the ring, and is kept at at temperature of 20 K. b is taken to be 19 mm, which is a value that has been corrected

$\omega_R/2\pi$ MHz	Q	$R_{\rm Res}$ MΩ/m
516.7	14171	6.88
612.2	18653	2.85
809.5	15611	2.99
880.3	27598	0.22
942.3	11651	1.29
1103.6	24819	2.21
1242.8	24584	0.001
1254.3	30227	0.001
1325.2	18386	0.27
1367.8	23835	0.001
362.5	16728	0.436
719.4	15933	0.027
748.6	15144	0.362
823.9	19147	0.464
1028.0	21034	1.040
1059.0	17836	0.197
1117.9	10016	1.821
1268.8	18071	0.327
1301.0	23277	0.196
1369.2	14922	2.439

Table 4: Computed septum cavity transverse higher order modes [5], per cavity. The cavity vessel is copper, the drift tube is stainless steel.

taking into account the beam pipe shape. We take t' to be 10 mm and t to be 50 μm. At these temperatures, $\rho = 1.8 \times 10^{-10}$ Ωm, and $\rho' = 5 \times 10^{-7}$ Ωm.

The remaining 10% of the ring is 2 mm thick copper at room temperature, giving a ρ of 1.5×10^{-8} Ωm. The correct formula is obtained by taking $t' = 0$. A simplified expression for the impedance in this case can be given by

$$-iR_1 \frac{\tanh(\sqrt{-i\omega/\omega_t})}{\sqrt{-i\omega/\omega_t}}, \tag{7}$$

where

$$R_1 = \frac{Z_0 L t}{\pi b^3} \qquad\qquad \omega_t = \frac{\rho}{\mu_0 t^2}. \tag{8}$$

In both cases, the average β-function is taken to be 85 m.

2.2 Narrow-Band Impedance

2.2.1 Septum cavities

The narrow-band impedance for each cavity consists of several resonators of the form (1), the parameters for which are given in Tab. 4. Since the modes are so narrow, it is possible that the precise value chosen for the mode frequency would cause the frequency where a line in the bunch spectrum overlaps the cavity mode to fall somewhere far away from the peak. Thus, in actual calculations, I reduce the Q for each cavity mode (where

$\omega_R/2\pi$ MHz	Q	$R_{\rm Res}$ MΩ/m
377.0318	52230	0.0143799959
405.9037	53717	0.0094233978
429.3622	54683	0.0029151936
449.9036	55736	0.0030414101
469.4352	56713	0.0036978174
487.8627	57187	0.0065667512
505.6887	58068	0.0041870586
522.8752	58606	0.0037995001
539.6390	59301	0.0019120649
555.9085	59556	0.0054062967
571.7696	59777	0.0074501183
587.1030	60033	0.0027672249
602.1747	60800	0.0027702037
617.1860	61819	0.0027162411
632.0662	62108	0.0104182498
646.6402	62320	0.0186548841
660.9645	62974	0.0014599614
675.1268	63830	0.0137874230
689.3647	63875	0.0321866830
703.4898	64191	0.0117533047
717.0502	65442	0.0256672155
730.9768	65460	0.0321239268
744.7866	66537	0.0073310018
758.4371	68721	0.0086235260
760.8246	97030	0.0138749352
772.2490	67989	0.0300684217
786.2016	69870	0.0111336881
796.7199	91030	0.0034391622

Table 5: Lower frequency computed higher order modes in the CMS experimental chamber [6]. Results are from `URMEL`.

necessary) to insure that the values for their associated multibunch growth rates will be at least 90% of their maximum possible values. Then, to account for this 90% factor, the $R_{\rm Res}$ are increased by a factor of 1/0.9.

The cavities have an average β-function of 200 m, and there are three of these cavities [5].

2.2.2 CMS experimental chamber

The narrow-band impedance for the CMS experimental chamber consists of several resonators of the form (1), the parameters for which are given in Tabs. 5 and 6. As with the cavity higher order modes, the modes for the CMS experimental chamber are so narrow that they must be broadened to insure that the correct values are obtained.

The average β-function is computed by taking the value of β at the IP (which is 0.5 m [2]) and assuming that the entire length of the chamber is treated as a drift. None

of the modes has a significant penetration to less than 8 m or more than 12 m. Thus, the average β-function is computed by averaging over that range; the result is 203 m.

2.3 Accelerating Cavities

The narrow-band impedance for the 8 accelerating cavities consists of several resonators of the form (1), the parameters for which are given in Tab. 7. The average β-function at the cavity is 150 m [8]; note that there is only one such set of 8 cavities.

3 Results

All the results in this section are obtained using the impedance model described in section 2. The computations are all done using the methods described in [1]. An updated version (version 0.1.2) of the program described in [9] was used to do the computation.

3.1 Injection

It is expected that the worst-case results will be at injection. Thus, I begin by giving results for that case.

3.1.1 Single Bunch

First, the single-bunch mode coupling threshold is computed. The mode-coupling threshold is 0.576 mA per bunch, corresponding to a total beam current of about 1.63 A (or 2.05 A for a symmetric fill). A plot of the mode frequencies versus current is shown in Fig. 2. The first modes to couple are the $m = 0$ (ω_y) and the $m = 1$ ($\omega_y - \omega_s$).

3.1.2 Multibunch Mode Growth Rates

The multibunch growth rates at the expected operating current of 0.536 A are given in Fig. 3. Note that the computation is done for a symmetric filling pattern. As described in [10, 1], if one does not have a symmetric filling pattern, one can take the bunch that has the highest current, and use it's current as the current for every bunch; this will give an upper bound on the growth rate (this statement should be qualified slightly; see [1] for a discussion). Thus, for this and all remaining multibunch computations in this paper, I multiply the real total current by M/k_B to get the current at which the computation is done. Thus, the plot in Fig. 3 is done at 0.674 A.

Figure 4 gives a way of determining which cavity modes generate individual peaks in Fig. 3 and subsequent figures.

3.1.3 Feedback

The transfer function for the proposed feedback system for the LHC can be described as a low-pass filter with a half-bandwidth of 730 kHz. Its response is thus described by the function

$$\frac{A}{1 - i\omega/\omega_{3\mathrm{db}}}, \tag{9}$$

where $\omega_{3\mathrm{db}} = 2\pi \cdot 730$ kHz. A is adjusted so that the maximum gain of all the multibunch modes will cancel a rise time of 10 ms. A particle receives a kick approximately two turns after the pickup sees it, at approximately the same point in the ring [11]. To get damping, I set the pickup to kicker distance to be 127.25 betatron oscillations (at the zero-current betatron frequency). See [1] for a discussion of how feedback is modeled.

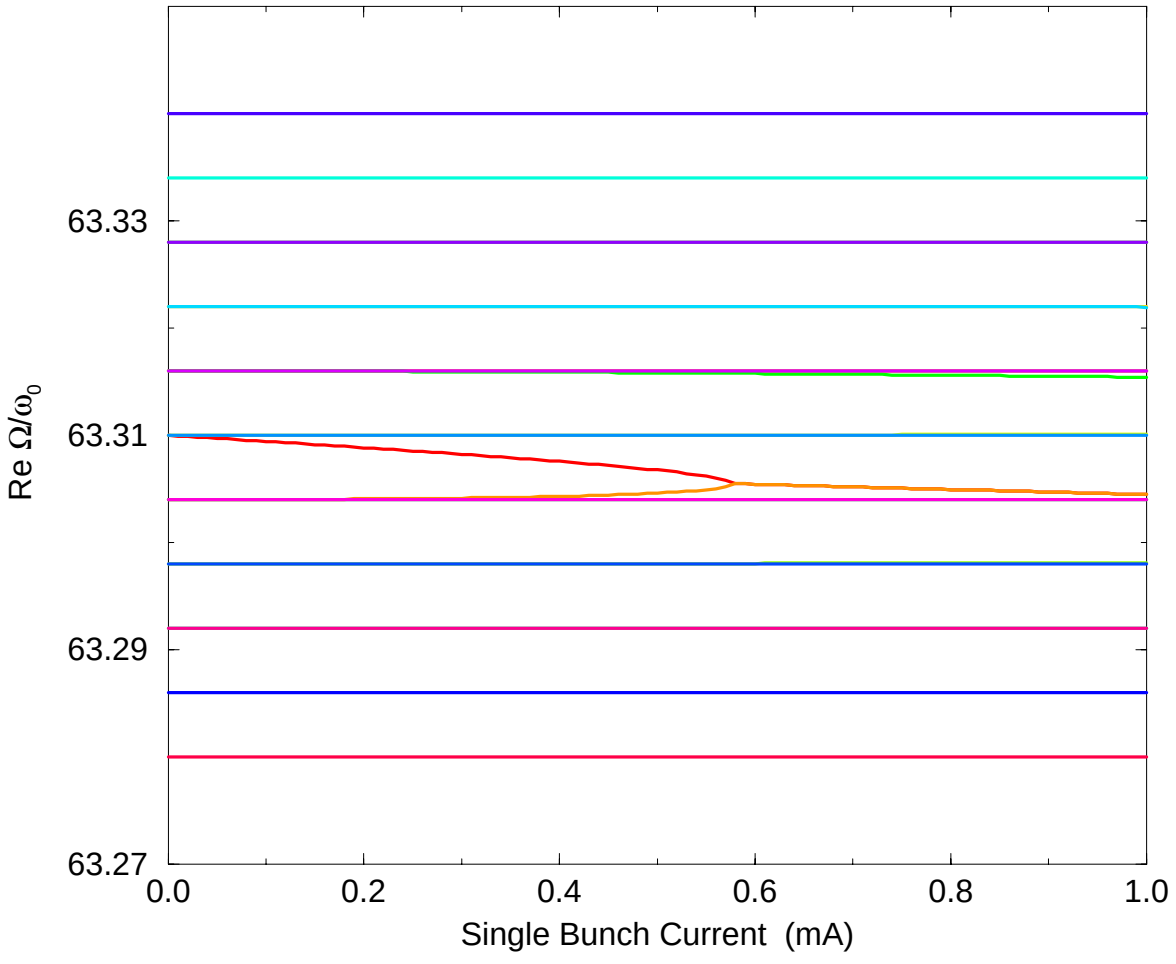

Figure 2: Mode frequencies versus single-bunch current for the LHC at injection. The lowest threshold is from coupling between the modes with zero-current frequencies of ω_y and $\omega_y - \omega_s$.

Figure 5 shows the effect of the feedback on the multibunch growth rates. It can be seen that many of the $m = 0$ modes that had large growth rates in Fig. 3 have been eliminated. However, Fig. 6 demonstrates that many of the $m = 0$ modes have not been eliminated. This is because the bandwidth of the feedback is very low, and thus its damping is over two orders of magnitude smaller than the peak damping rate for some of the $m = 0$ multibunch modes. In fact, Fig. 6 indicates that the insufficiently damped modes are not only from cavity modes, but also from the resistive wall impedance.

The feedback damped only 49% of the highest peak shown in Fig. 6. Thus, since in the high-frequency tail of the feedback response (9), the real part of the transfer function is proportional to $\omega_{3\mathrm{db}}^2$, increasing the bandwidth by a little over a factor of 1.4 should be sufficient to damp all of the modes. It turns out, for reasons possibly related to mode coupling, that it is necessary to increase the bandwidth by a factor of two to damp all the $m = 0$ modes. Once this is done, the growth rates look like those shown in Fig. 7.

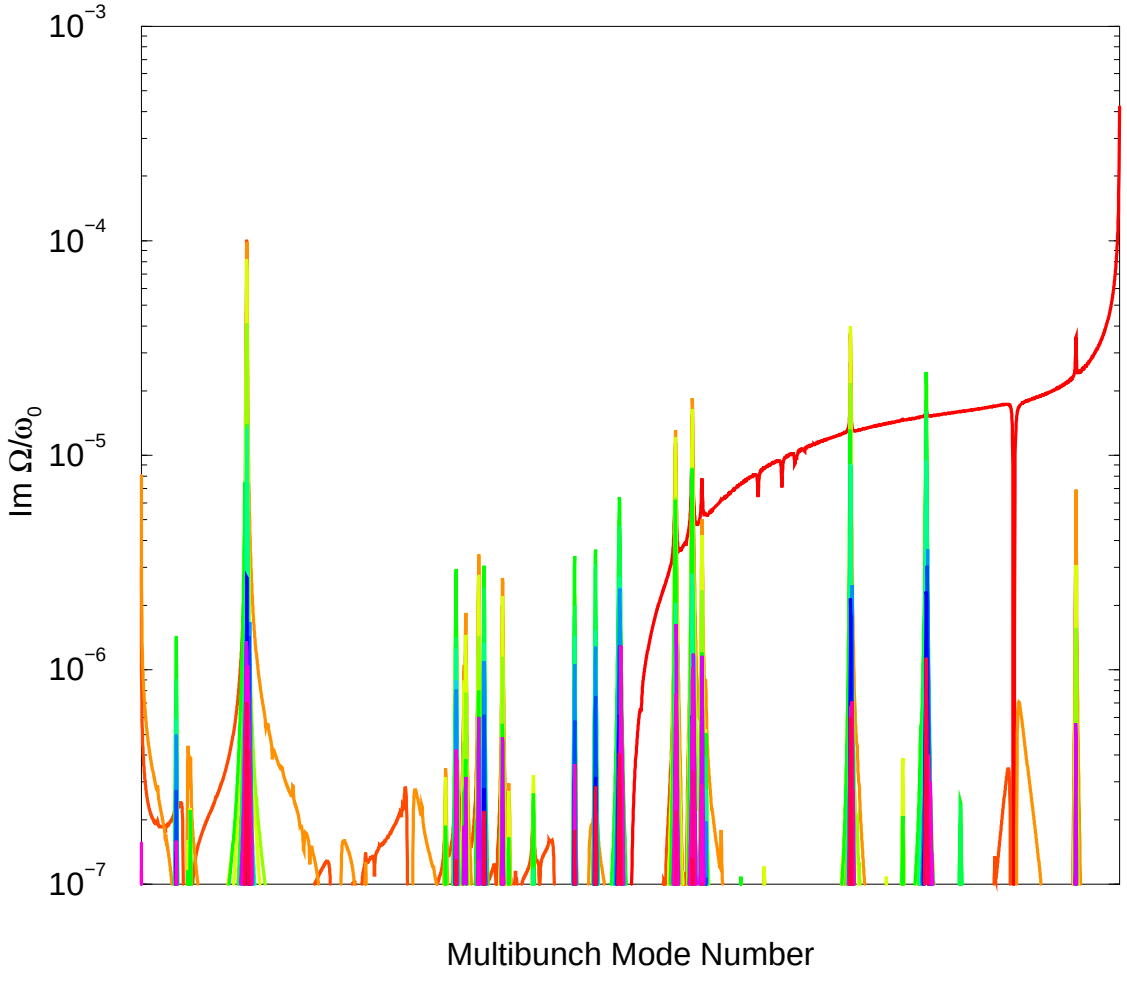

Figure 3: Growth rates of multibunch modes for the LHC at injection. The value of the growth rate is plotted versus the multibunch mode number. The plot consists of several lines, one for each type of internal-bunch motion. Each line is really M separate points connected by a line, one point for each multibunch mode. The computation is done for M symmetrically placed bunches, with a total beam current of $IM/k_B = 0.674$ A. The large peak on the left side of the figure is primarily caused by two of the septum cavity higher order modes: the one at 516.7 MHz, and the one at 1117.9 MHz (see Tab. 4 and Fig. 4). The peak all the way to the right of the figure is primarily caused by the resistive-wall impedance.

3.1.4 Multibunch Mode Coupling

When one only considers a single bunch, one finds that the growth rates sharply increase at the current where the modes frequencies coincide. If the growth rates for multibunch modes are plotted versus current, they display similar behavior. In some cases, however, the current where they sharply increase is lower than the current calculated for a single bunch (multiplied by the number of bunches).

Figures 8 and 9 show the growth rates of the $m = 1$ modes plotted versus current for two different subsets of the multibunch modes. The resistive wall impedance decreases what one might call the mode coupling threshold by a significant amount, as can be seen from Fig. 8. The threshold now seems to be around 1.5 A or so, which would correspond

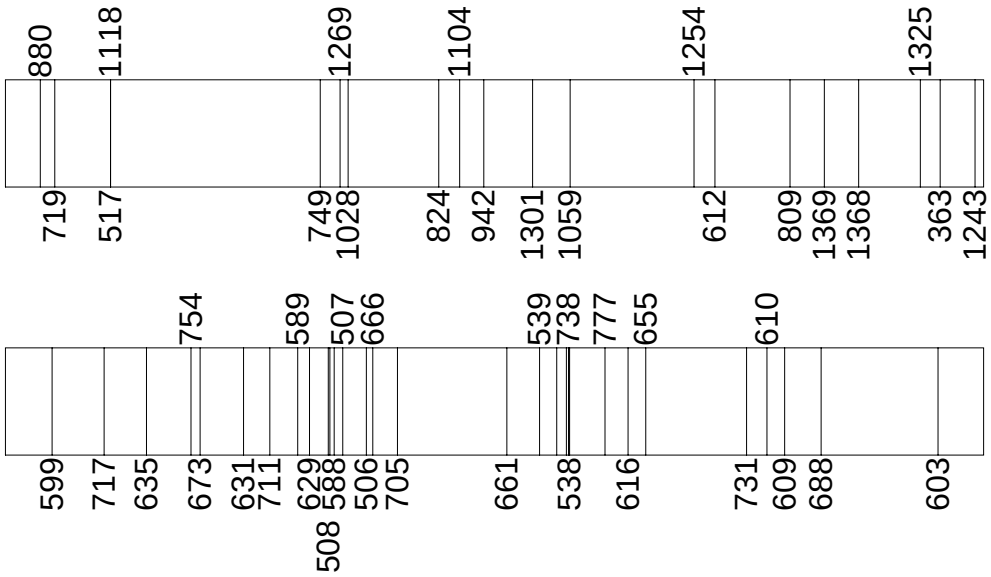

Figure 4: Aid for determining the source of peaks in Fig. 3 and subsequent figures. Each vertical line represents one of the cavity higher order modes given in Tabs. 4 and 7. Each line is labeled with the frequency in megahertz of the associated cavity mode. The lower set are from the accelerating cavities, the upper set are from the septum cavities.

to 1.2 A for the actual filling.

If feedback is included, these results get somewhat worse. I will use the 1460 kHz half-bandwidth feedback described above. Figures 10 and 11 show the results. The point where the growth rates start to increase in Fig. 10 is about the same as it was without feedback as shown in Fig. 8. However, in Fig. 11, notice that the sharp increase occurs at a significantly lower current than it did without feedback (compare Fig. 9). The reason for this is that the transfer function for the feedback described in Eq. (9) has a non-zero imaginary part. This imaginary part causes a shift in the frequencies of the multibunch modes, causing the modes to intersect at currents that are lower than usual. A different set of modes gives worst behavior in the presence of feedback; they are shown in Fig. 12.

3.2 Collision

At collision, the constraints will probably be less severe due to the increased energy. However, there are four factors which make it necessary to do the computation:

- As described in subsection 2.1.1, the space charge impedance decreases at the higher energy, giving a net increase in the inductive impedance (the space charge cancels some of the inductive impedance).
- The bunch length decreases, potentially increasing the $m = 0$ mode complex frequency shifts in particular.
- The synchrotron frequency decreases, potentially lowering the mode coupling threshold.
- To maintain the same gain, more feedback power is required. This issue will not be addressed here, however.

It turns out that the single bunch mode coupling threshold is around 2.0 mA per bunch, and that multibunch mode coupling does not give a significantly lower threshold.

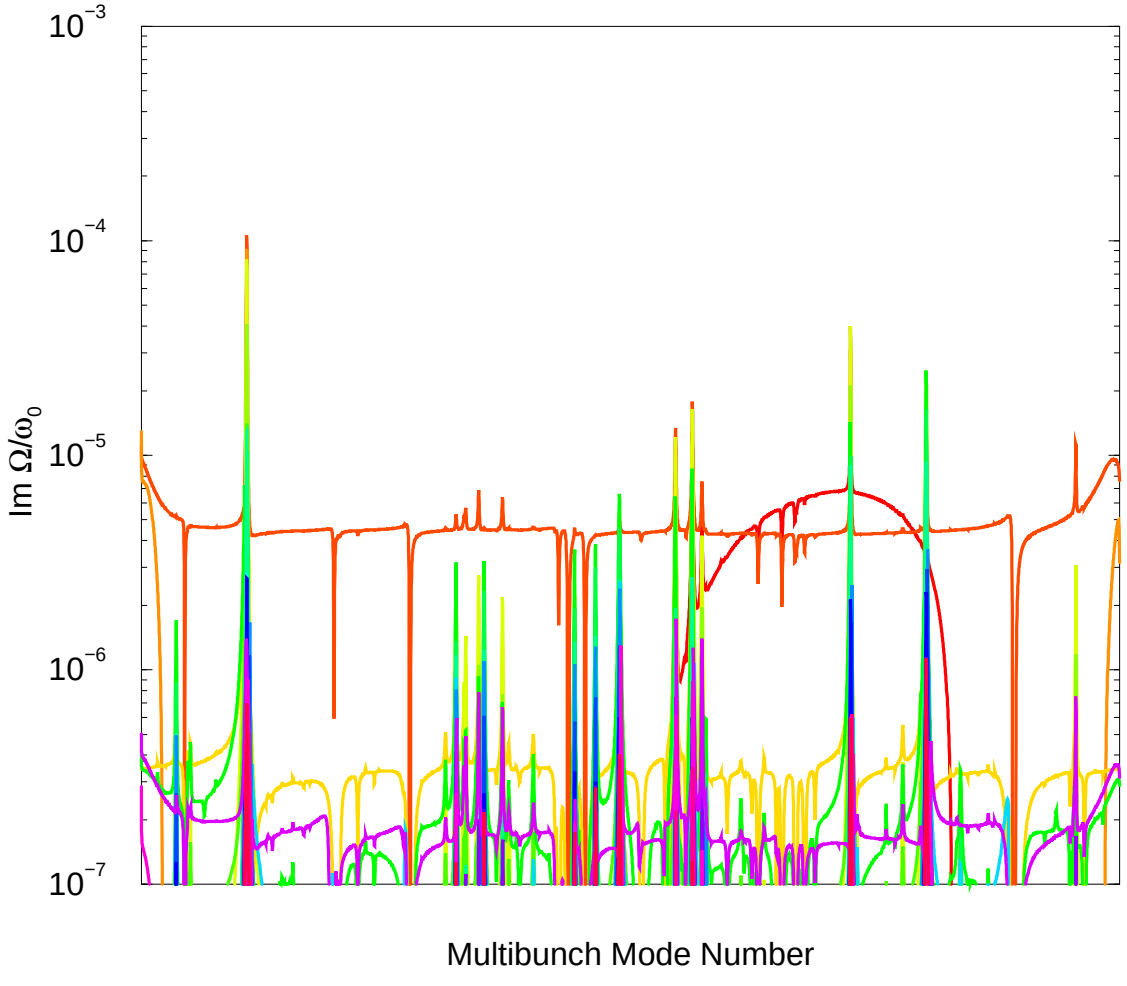

Figure 5: Growth rates of multibunch modes at injection, with feedback.

Thus, the behavior at injection determines the thresholds from these types of effects.

Figure 13 shows the growth rates for the multibunch modes without feedback. Figure 14 shows them with the wide (1460 kHz) feedback proposed above (using the same gain as above). As can be seen from examining Fig. 15, some of the multibunch modes are missed by this feedback, probably because of the bunch shortening.

The feedback seems to have insufficient gain to damp some of the $m = 0$ multibunch modes. As before, this could be fixed with either a wider bandwidth or more gain. Carefully comparing Figs. 15 and 13, one sees that the 612.2 MHz cavity mode is only damped to 73% of its undamped value. Even though the peak coming from the 516.7 MHz and 1117.9 MHz is a bit higher in Fig. 15 than the peak from the 612.2 MHz mode, it is damped down to 22% of it's value. Thus, a further increase in bandwidth or gain is necessary to correct these modes.

4 Conclusions

The threshold for transverse mode coupling for multibunch modes is above the desired operating threshold by about a factor of two. We should thus examine our impedance model more carefully since this threshold is so close to the operating current. The bandwidth of the feedback as it stands seems insufficient to damp all of the $m = 0$ modes.

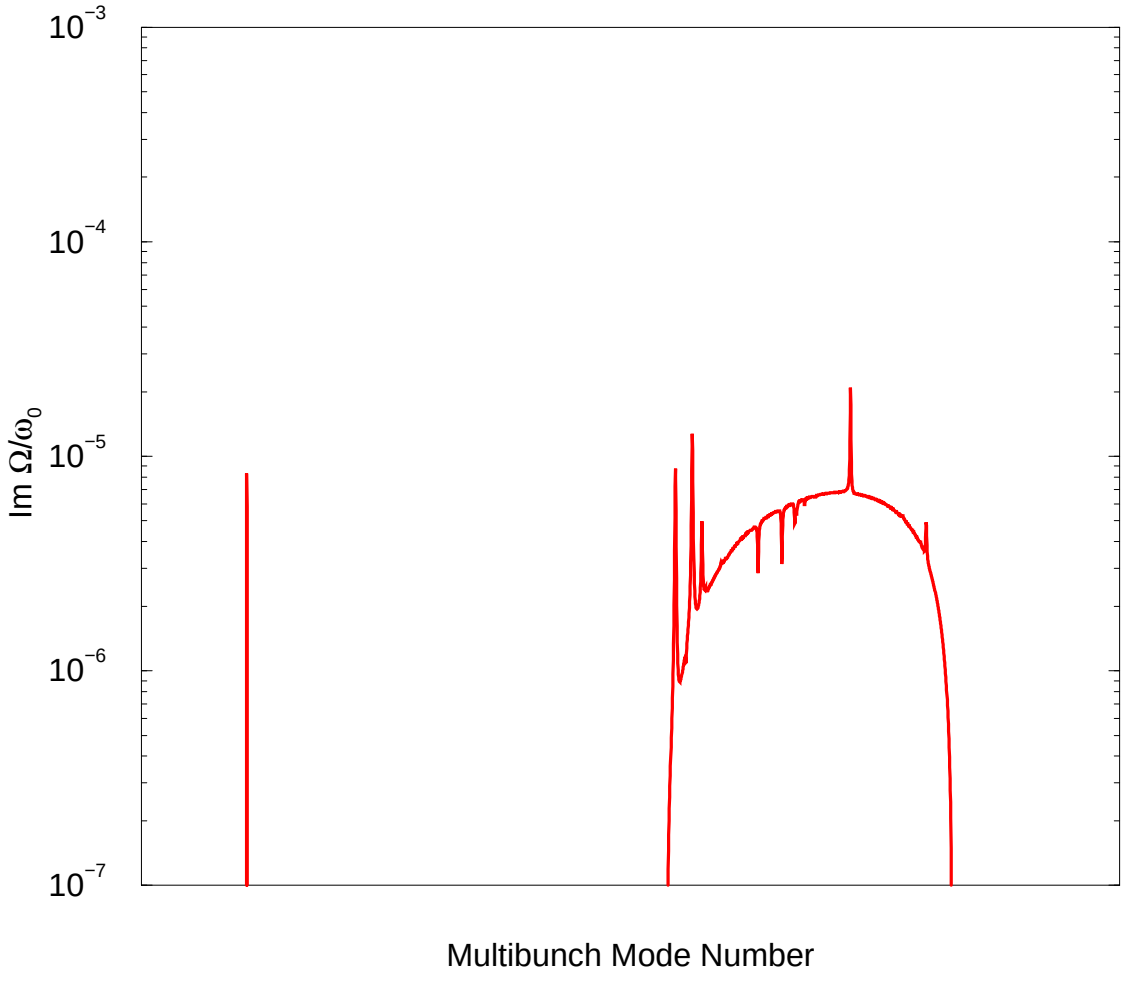

Figure 6: Growth rates of $m = 0$ multibunch modes at injection, with feedback.

Increasing the bandwidth by a factor of two or so should probably be able to damp all of the modes at injection. However, compared to injection, the feedback at collision needs a significantly larger gain (or a larger bandwidth).

In some cases, the multibunch modes may be stable from Landau damping due to the presence of tune shift with amplitude. This tune shift with amplitude can be in the transverse plane, from octupoles for instance, or in the longitudinal plane, from nonlinearity in the r.f. voltage or potential-well distortion. Note that tune shift with amplitude in the longitudinal plane cannot help the $m = 0$ transverse modes. Calculation of the extent of Landau damping is in progress, and the results are not presented here.

5 Acknowledgments

Many people have contributed to this computation. Francesco Ruggiero helped greatly by talking to the right people to obtain information about the machine impedances and parameters. Wolfgang Höfle, Oliver Brüning, Volker Rödel, and Trevor Linnecar supplied many of the impedance parameters that were needed for this calculation, outside of those of Ruggiero in [3].

I benefited from discussions with Francesco Ruggiero and Bruno Zotter which prompted a careful recomputation of Landau damping due to longitudinal tune shift

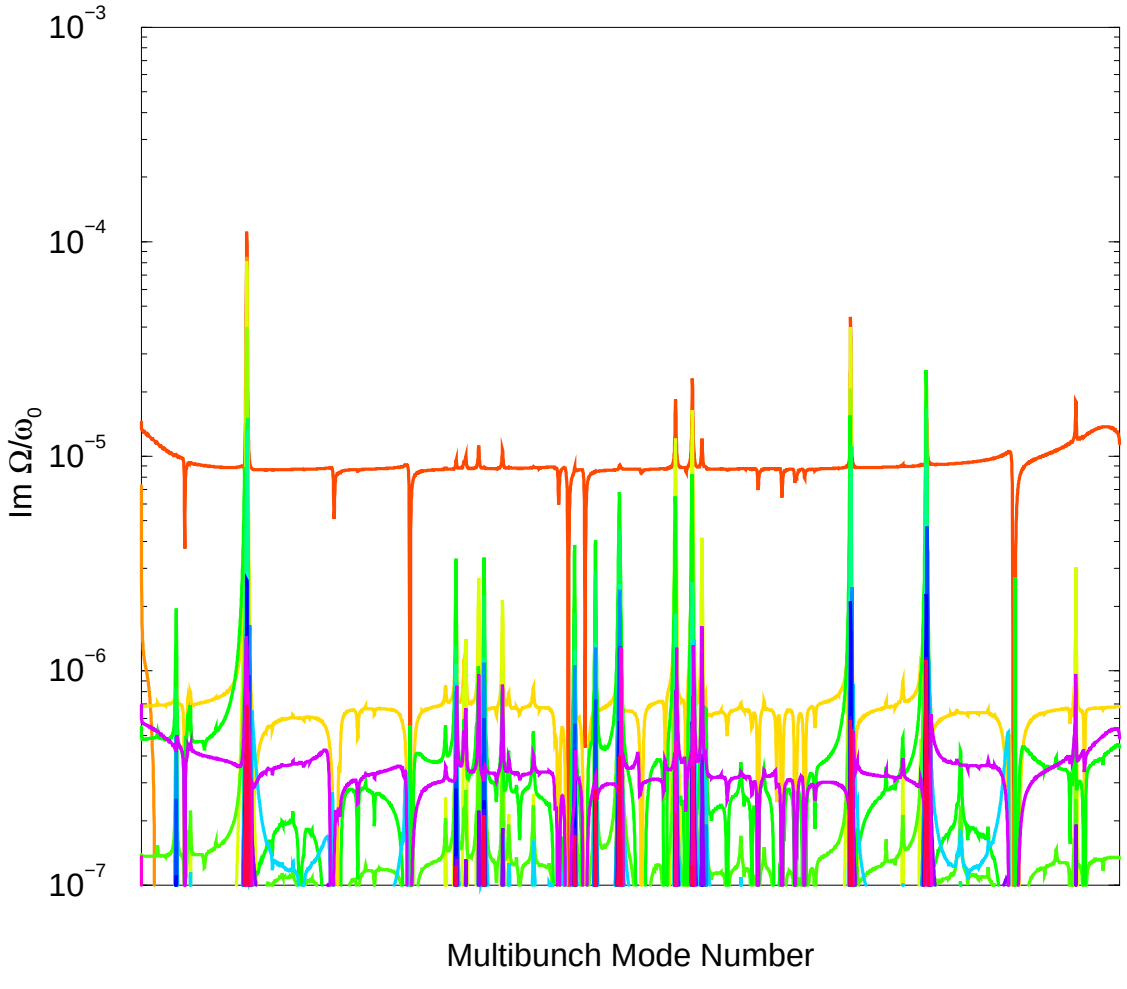

Figure 7: Growth rates of multibunch modes at injection, with feedback having a half bandwidth of 1460 kHz. All $m = 0$ modes are damped.

with amplitude, the results of which have prompted me to defer a discussion of Landau damping to a later paper.

Francesco Ruggiero has helped greatly with suggestions for and comments on the content of this paper, and has helped to greatly improve the quality of the resulting document.

Finally, this work would not be possible were it not for the generous funding that I have received from CERN. Also, much of the basis for this work [1] was done at SLAC under the auspices of the United States Department of Energy, contract number DE–AC03–76SF00515.

References

[1] J. Scott Berg. *Coherent Modes for Multiple Non-Rigid Bunches in a Storage Ring*. PhD thesis, Stanford University, Stanford, CA, March 1996. SLAC report SLAC-R-478.

[2] The LHC Study Group. The large hadron collider, conceptual design. Technical Report CERN/AC/95-05(LHC), CERN, Geneva, Switzerland, October 1995.

[3] Francesco Ruggiero. Single-beam collective effects in the LHC. Technical Report

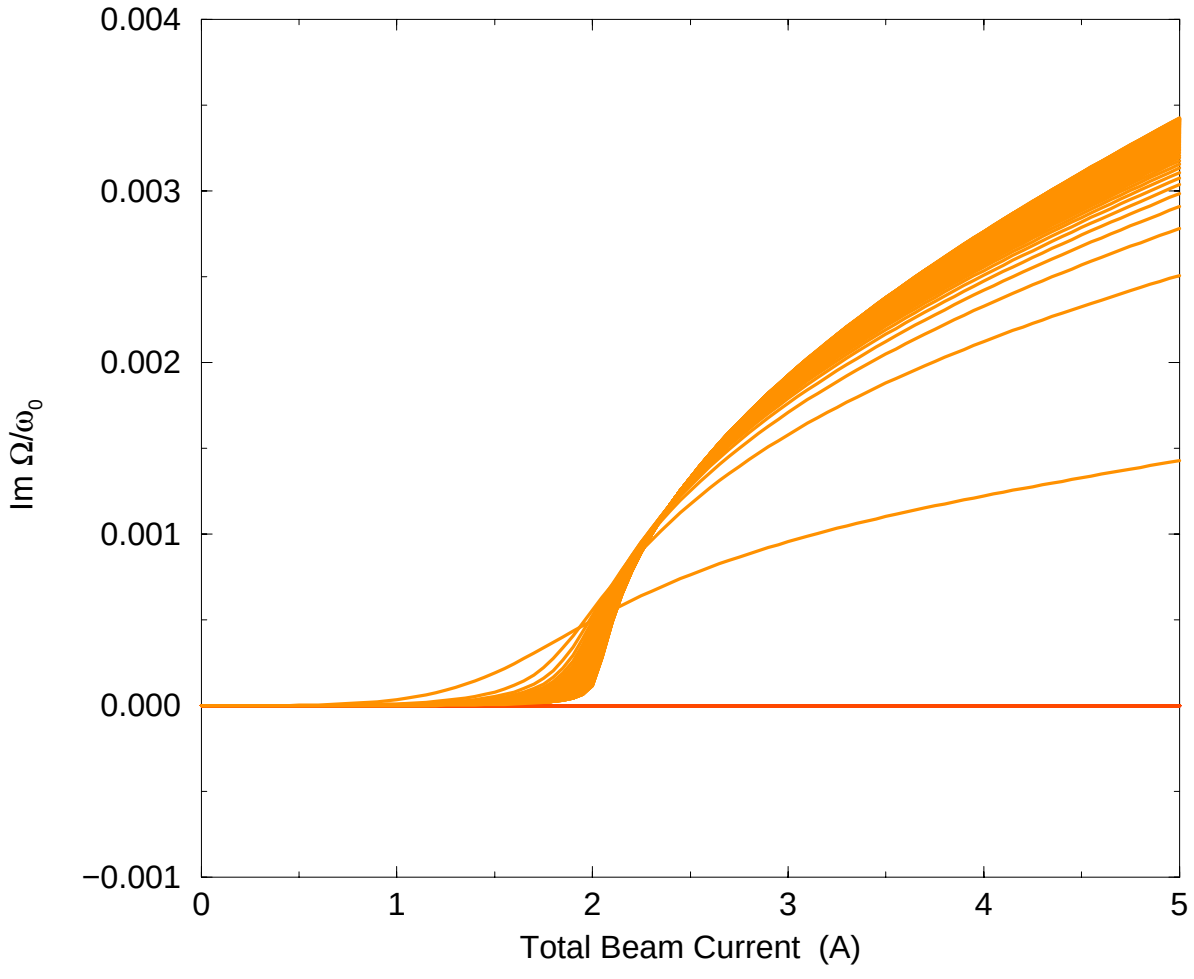

Figure 8: Growth rates of $m = 1$ multibunch modes at injection plotted versus total beam current. This is a subset of all the $m = 1$ multibunch modes. The worst mode in this set is driven by the resistive wall impedance.

CERN SL/95-09 (AP), CERN, Geneva, Switzerland, February 1995. Presented at the Workshop on Large Hadron Colliders, Montreux, Switzerland, October 1994.

[4] Wolfgang Höfle, April 1996. Informal meeting at CERN, 11 April 1996.

[5] Wolfgang Höfle, May 1996. Private communication.

[6] Oliver Brüning, April 1996. Private communication.

[7] V. Rödel. Private communication.

[8] Francesco Ruggiero, May 1996. Private communication.

[9] J. Scott Berg. Documentation for `vlasov` version 0.1. Technical Report SLAC-TN-96-1, SLAC, Stanford, CA, March 1996.

[10] R. D. Kohaupt. On multi-bunch instabilities for fractionally filled rings. Technical Report DESY-85-139, DESY, Hamburg, Germany, December 1985.

[11] Wolfgang Höfle and T. Linnecar, May 1996. Private communication.

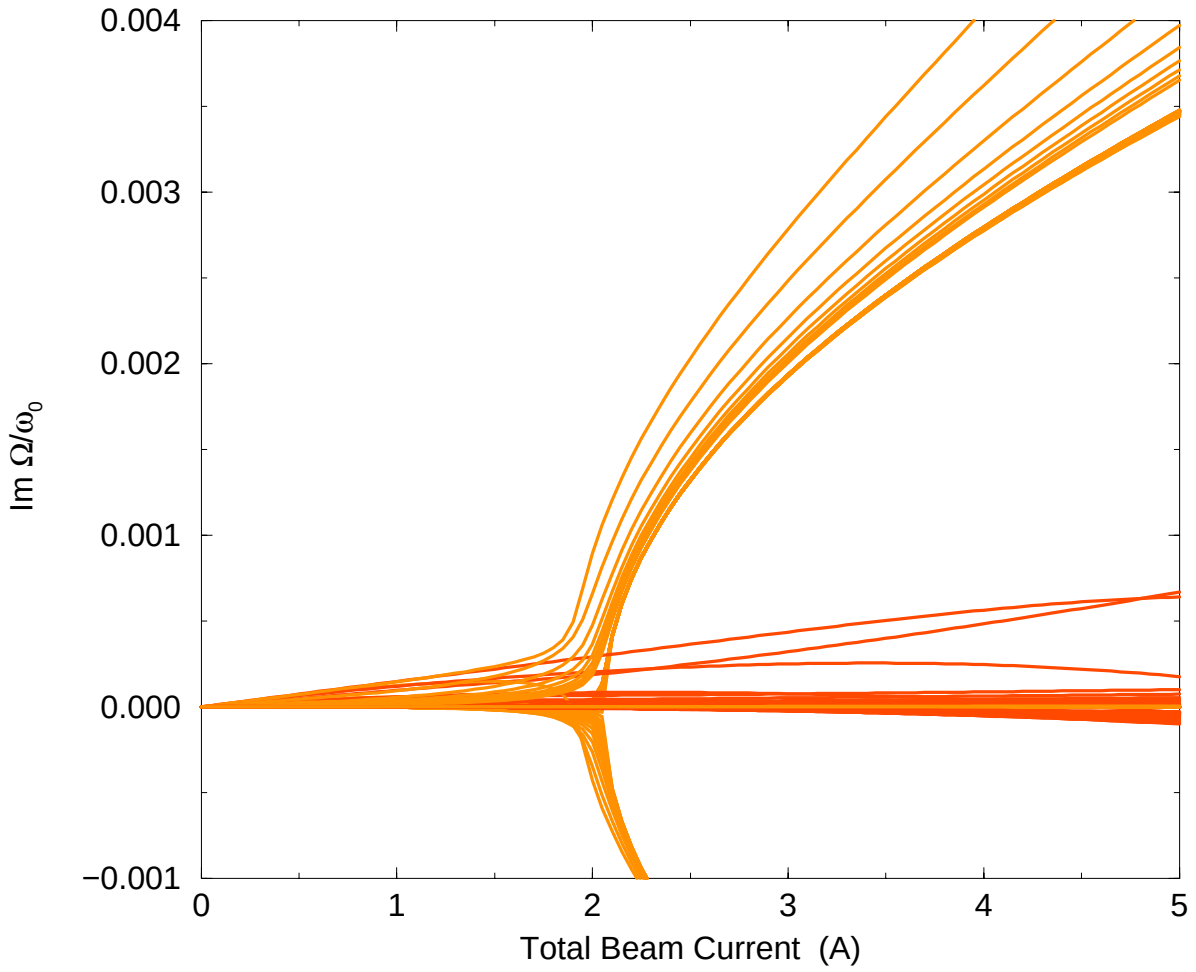

Figure 9: Growth rates of $m = 1$ multibunch modes at injection plotted versus total beam current. This is a subset of all the $m = 1$ multibunch modes. The worst mode in this set is driven by one of the cavity higher order modes.

$\omega_R/2\pi$ MHz	Q	R_{Res} MΩ/m
806.178725	65718	0.0032314156
819.914840	66181	0.0024767592
827.934807	98326	0.0011779502
833.735978	66372	0.0030504240
847.464128	66886	0.0032327712
853.857491	98127	0.0004833148
861.109509	67139	0.0039772346
874.735214	68039	0.0028151592
877.122400	96832	0.0016194240
888.354748	68161	0.0029541638
898.781637	97071	0.0017999568
902.084016	68529	0.0024503738
915.710966	69116	0.0024360108
919.906951	97091	0.0023059004
929.256448	69084	0.0023702604
940.406590	96883	0.0007463622
942.852344	69417	0.0030562996
956.208720	69322	0.0031899786
960.086981	96813	0.0000710126
969.702617	69144	0.0033781084
978.861948	96529	0.0012577822
983.002134	69721	0.0029960980
996.157673	71110	0.0028917486
997.347061	93734	0.0013455842
1009.572220	70450	0.0031873408
1015.499440	95964	0.0026448550
1022.798870	70802	0.0036858574
1033.522250	95513	0.0003260078
1036.178940	70969	0.0029908172
1049.264510	71559	0.0025464756
1051.242180	96305	0.0014850864
1052.885920	120708	0.0000197992
1062.376810	70873	0.0030326952
1068.549400	95813	0.0013069240
1075.594290	71477	0.0028170786
1085.772260	95128	0.0017314676
1088.652340	72267	0.0027906538
1092.715920	124699	0.0000760940
1101.758030	73338	0.0014019066
1102.958140	92769	0.0021970440
1114.881450	72463	0.0033082536
1119.587080	95290	0.0007429384

Table 6: Lower frequency computed higher order modes in the CMS experimental chamber [6]. Results are from `MAFIA`.

$\omega_R/2\pi$ MHz	Q	$R_{\rm Res}$ MΩ/m
506.222	10000	0.7554
507.198	10000	0.9758
507.729	10000	0.4664
507.802	10000	0.2480
537.990	10000	0.0734
538.128	10000	1.3782
538.522	10000	5.3099
539.216	10000	3.9492
587.708	10000	0.0067
589.205	10000	0.0019
599.267	10000	0.0853
603.056	10000	0.0567
609.325	10000	0.1002
610.064	10000	0.1281
615.744	10000	0.0520
628.791	10000	0.1086
631.491	10000	0.0032
635.484	10000	0.0099
655.107	10000	0.0217
660.790	10000	0.0273
666.278	10000	0.0989
673.361	10000	0.2489
688.001	10000	0.0228
705.355	10000	0.1478
710.588	10000	0.0547
717.371	10000	0.0084
731.140	10000	0.0012
738.429	10000	0.0169
753.893	10000	0.0003
777.012	10000	0.0635

Table 7: Higher order modes for the accelerating cavities, for the set of 8 cavities [7]. Q values are taken arbitrarily to be 10000 [8].

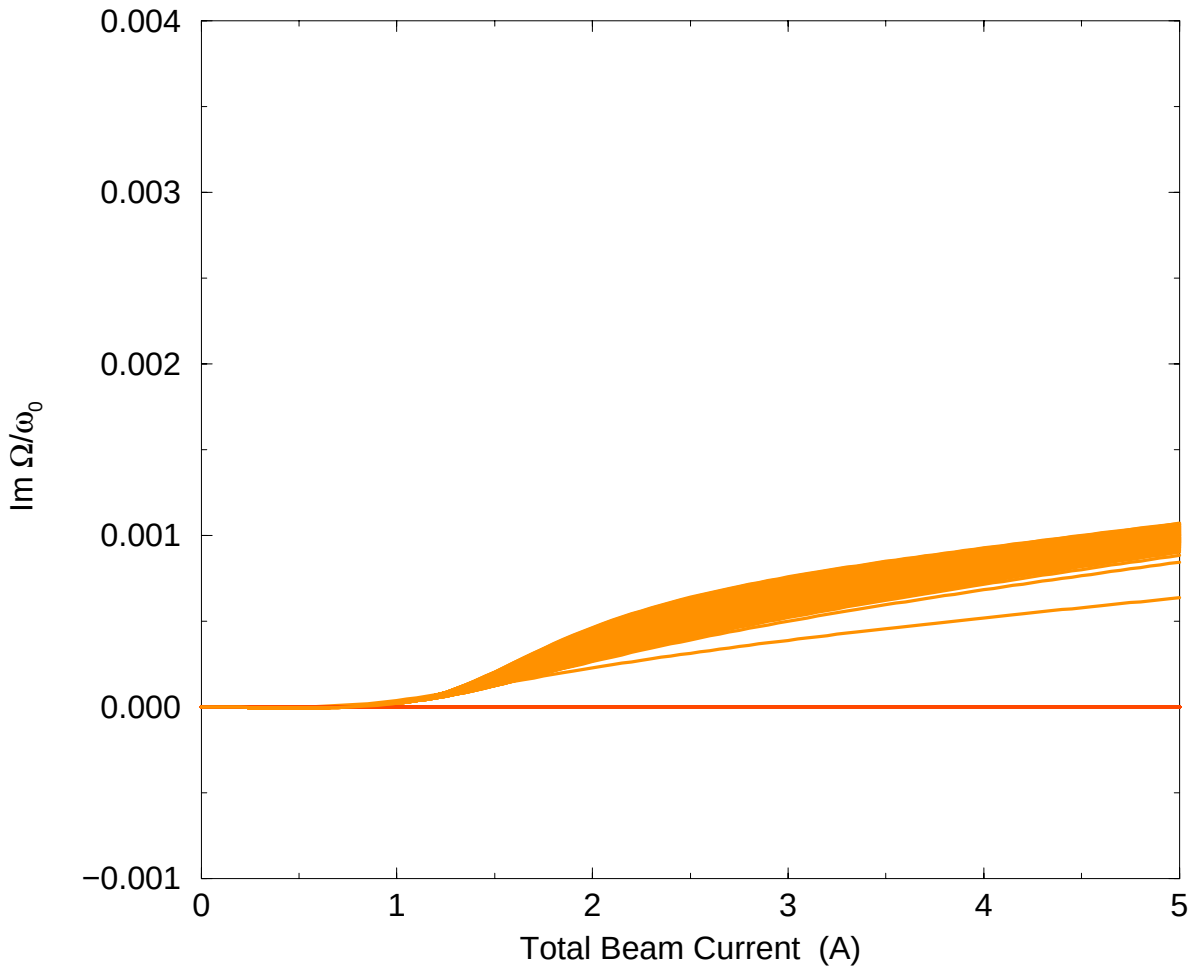

Figure 10: Growth rates of $m = 1$ multibunch modes at injection with feedback plotted versus total beam current. These are the same subset of modes as were shown in Fig. 8.

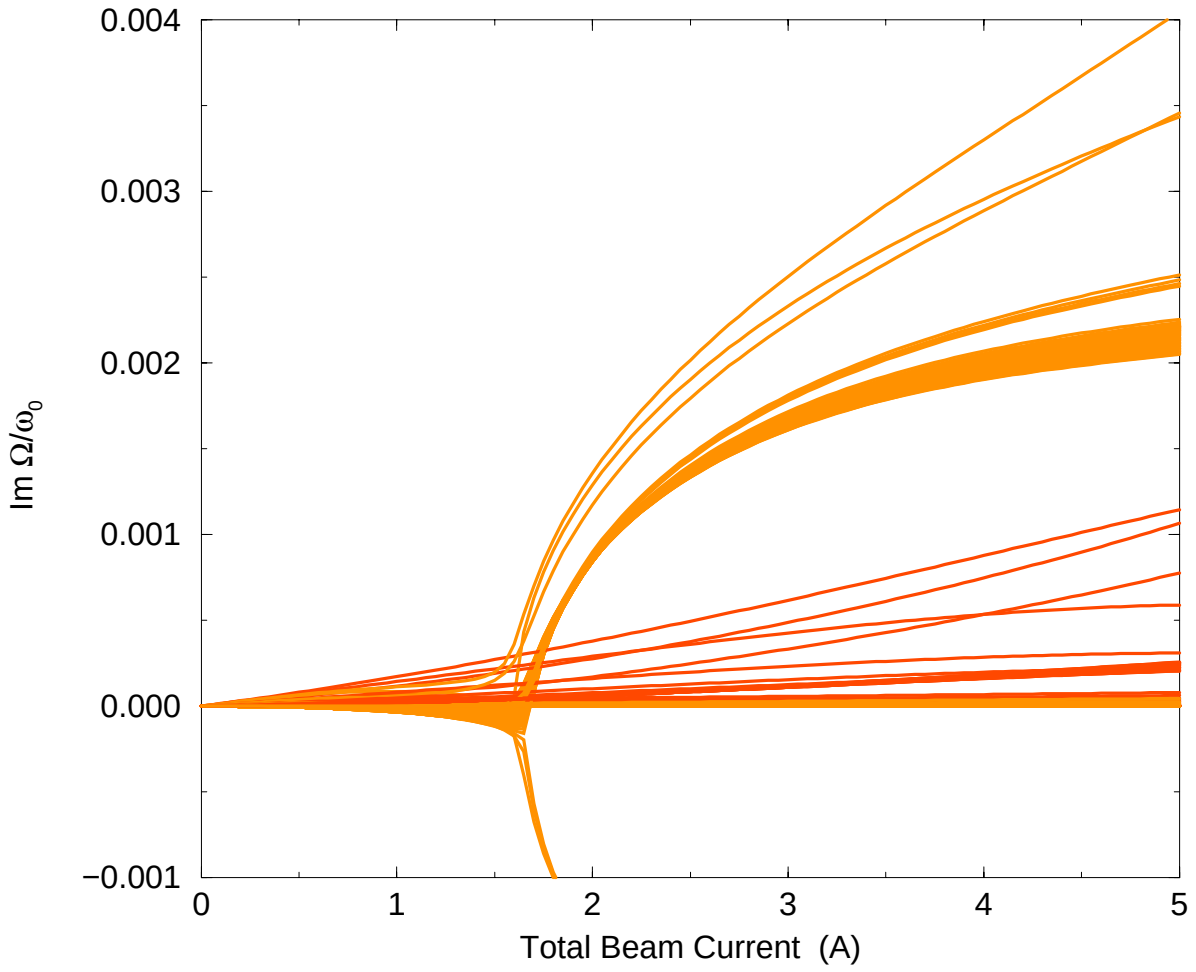

Figure 11: Growth rates of $m = 1$ multibunch modes at injection with feedback plotted versus total beam current. These are the same subset of modes as were shown in Fig. 9.

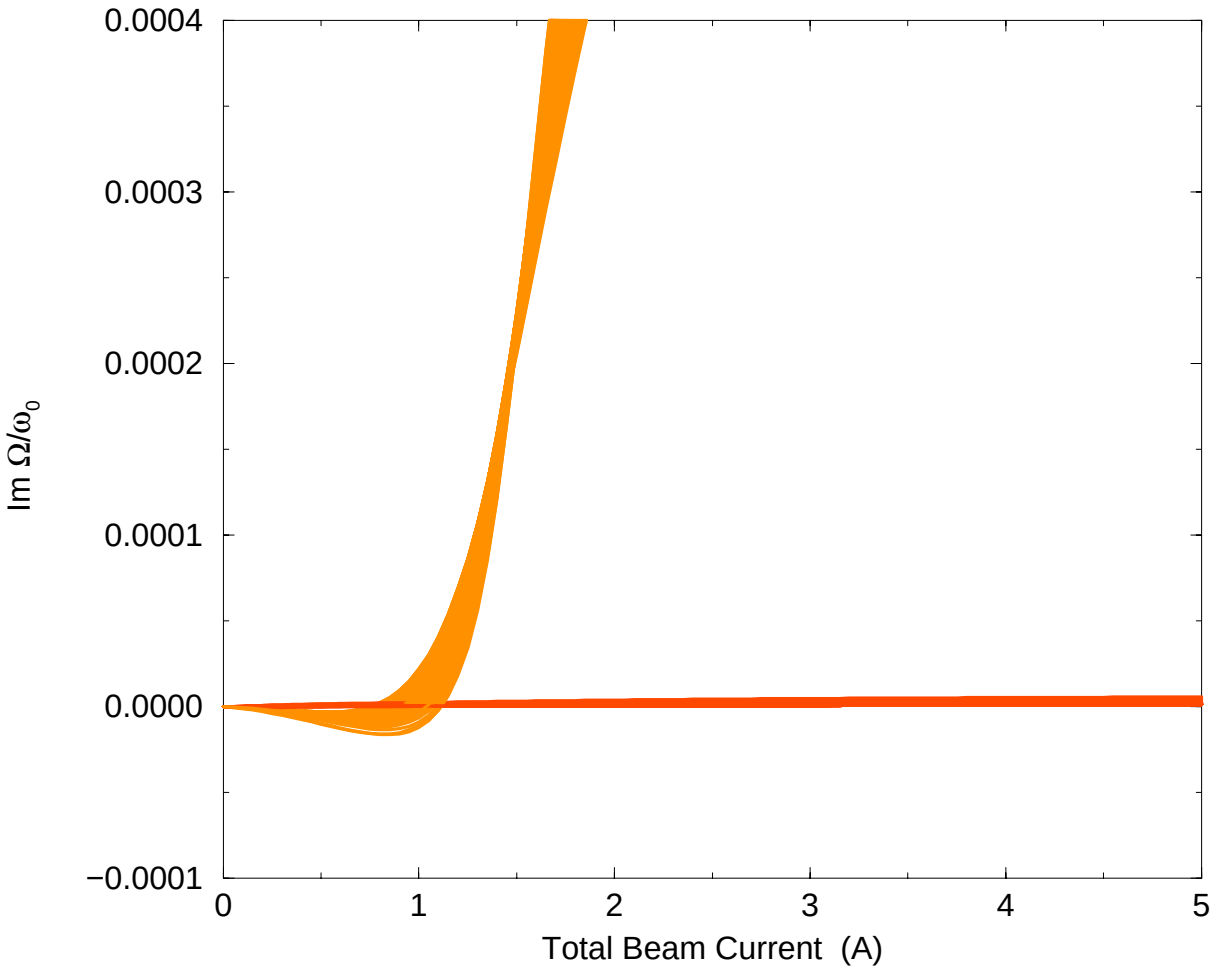

Figure 12: Growth rates of $m = 1$ multibunch modes at injection with feedback plotted versus total beam current. This is the worst group of modes in the presence of feedback. Note that the vertical scale is a factor of 10 smaller than in previous figures, so as to show more detail of the region where the growth rates are beginning to increase.

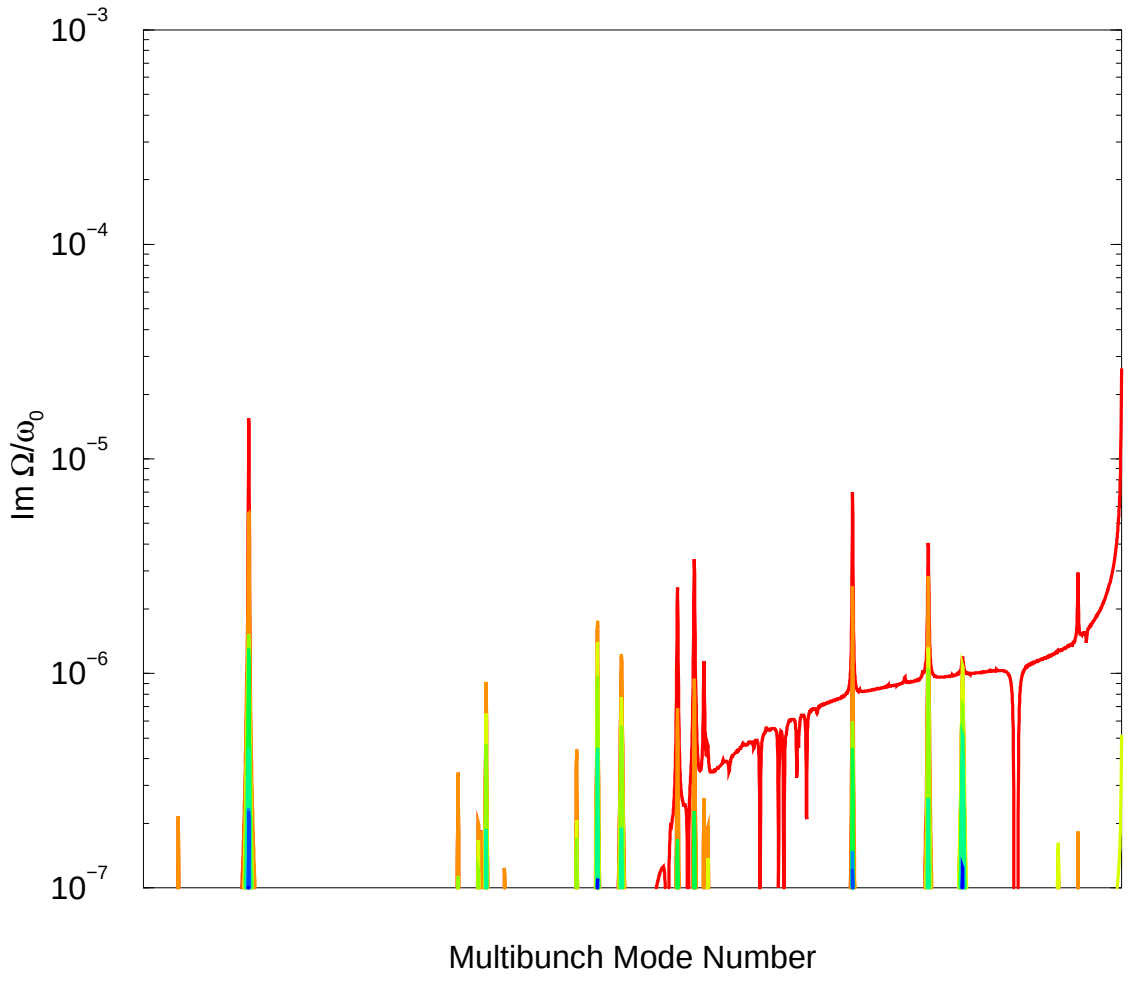

Figure 13: Growth rates of multibunch modes for the LHC at collision.

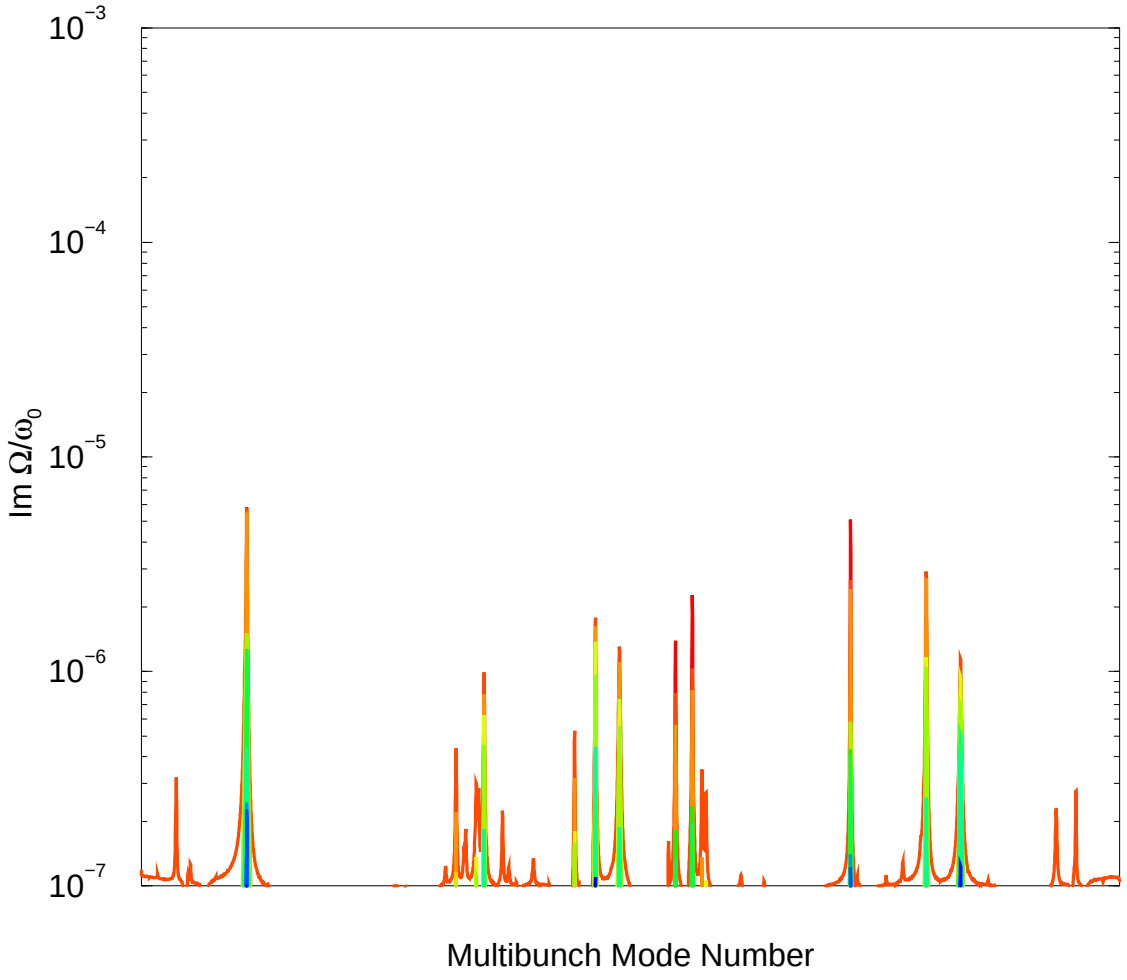

Figure 14: Growth rates of multibunch modes for the LHC at collision, with 1460 kHz half-bandwidth feedback.

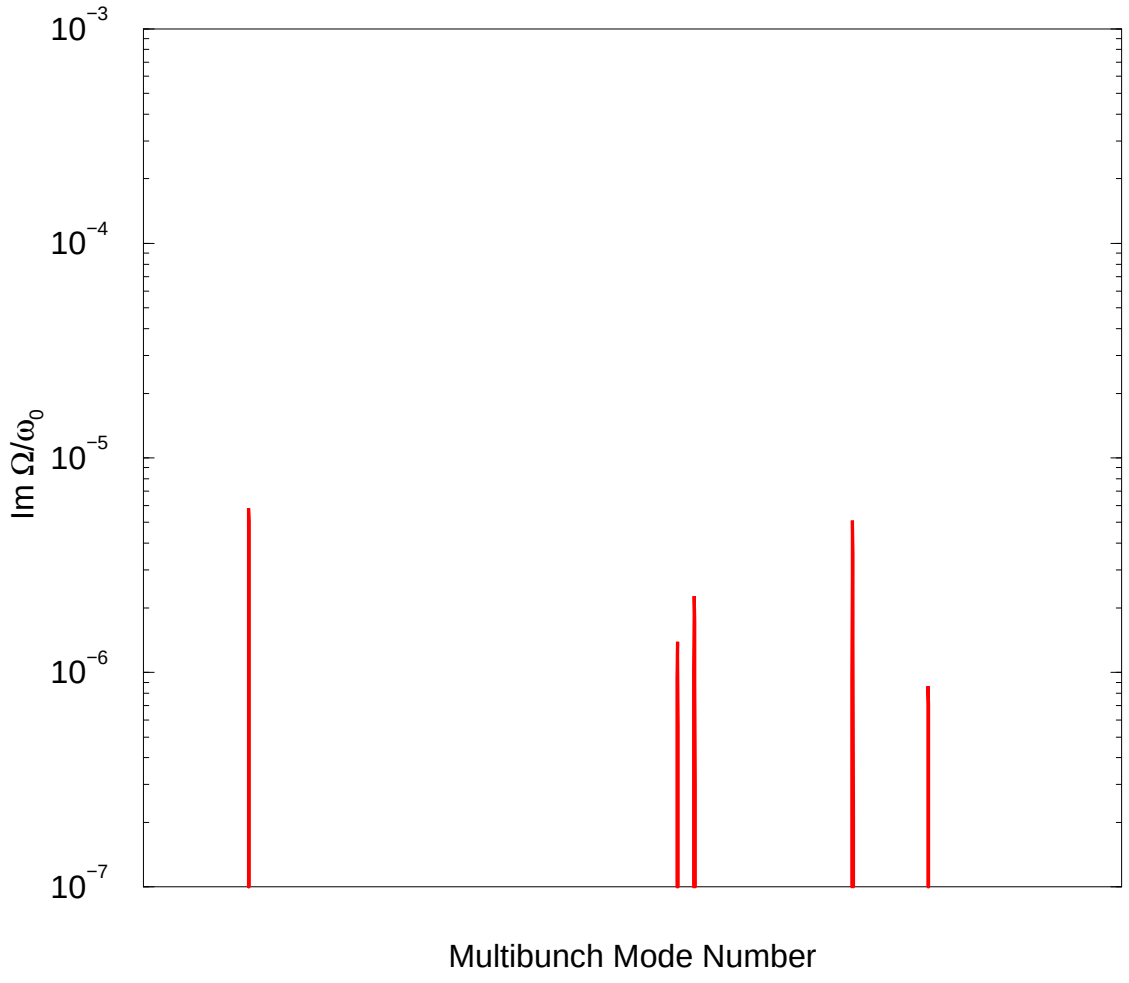

Figure 15: Figure 14, showing only the $m = 0$ multibunch modes.